



Monodisperse magnetite (Fe_3O_4) nanoparticles modified with water soluble polymers for the diagnosis of breast cancer by MRI method



Ali Hossein Rezayan^{a,*}, Majid Mousavi^a, Somayyeh Kheirjou^b, Ghasem Amoabediny^c, Mehdi Shafiee Ardestani^d, Javad Mohammadnejad^a

^a Department of Life Science Engineering, Faculty of New Sciences and Technologies, University of Tehran, Tehran, Iran

^b Department of Chemistry, Sharif University of Technology, Tehran, Iran

^c School of Chemical Engineering, College of Engineering, University of Tehran, Tehran, Iran

^d Department of Pharmacy, Tehran University of Medical Sciences, Tehran, Iran

ARTICLE INFO

Article history:

Received 10 January 2016

Received in revised form

11 June 2016

Accepted 1 July 2016

Available online 2 July 2016

Keywords:

Nanoparticles

Magnetic materials

PEGdiacid-modified Fe_3O_4 nanoparticles

MRI

ABSTRACT

In this study, magnetic nanoparticles (MNPs) were synthesized via co-precipitation method. To enhance the biocompatibility and colloidal stability of the synthesized nanoparticles, they were modified with carboxyl functionalized PEG via dopamine (DPA) linker. Both modified and unmodified Fe_3O_4 nanoparticles exhibited super paramagnetic behavior (particle size below 20 nm). The saturation magnetization (M_s) of PEGdiacid-modified Fe_3O_4 was 45 emu/g, which was less than the unmodified Fe_3O_4 nanoparticles (70 emu/g). This difference indicated that PEGdiacid polymer was immobilized on the surface of Fe_3O_4 nanoparticles successfully. To evaluate the efficiency of the resulting nanoparticles as contrast agents for magnetic resonance imaging (MRI), different concentration of MNPs and different value of echo time TE were investigated. The results showed that by increasing the concentration of the nanoparticles, transverse relaxation time (T_2) decreased, which subsequently resulted in MR signal enhancement. T_2 -weighted MR images of the different concentration of MNPs in different value of echo time TE indicated that MR signal intensity increased with increase in TE value up to 66 and then remained constant. The cytotoxicity effect of the modified and unmodified nanoparticles was evaluated in three different concentrations (12, 60 and 312 mg l^{-1}) on MDA-MB-231 cancer cells for 24 and 48 h. In both tested time (24 and 48 h) for all three samples, the modified nanoparticles had long life time than unmodified nanoparticles. Cellular uptake of modified MNPs was 80% and reduced to 9% by the unmodified MNPs.

© 2016 Elsevier B.V. All rights reserved.

1. Introduction

Diseases, especially cancers are currently the most important problem of humanity. Breast cancer is one of the most common types. The determination of breast cancer at early stage could be the key to successful treatment. Despite the availability and prevalence of mammography imaging, there is still additional benefit to be gained from the additional screening methodologies. Regarding the fact that the tumors have very small size at the initial stage, recent researchers have found that Magnetic Resonance Imaging (MRI) can detect some small breast lesions sometimes missed by mammography. It can also help to detect breast cancer in women with breast implants and in younger women who tend to have dense breast tissue [1,2]. MRI is the most brighting safe diagnostic technique used in the diagnosis and treatment of

medical conditions in medicine [3,4]. One of the disadvantages of MRI is the low resolution and quality of the resulted image. An alternative solution to this problem is the use of efficient contrast agent. Contrast agent could be of paramagnetic or super paramagnetic material such as iron oxides [4].

However, it has been recognized that the iron oxide nanoparticles could be good successor for their normal size counterpart [5–8]. Fe_3O_4 nanoparticles have been tested vigorously for various biomedical applications in view of their chemical stability and environmentally friendly, with good storage and operation stability [9]. Moreover, the use of iron oxide nanoparticles can also be more effective in the treatment of breast cancer. Their susceptibility to being operated under a magnetic field, provides them as controllable tools for magnetically tagging of biomolecules or cells, which result in highly efficient bioseparation, drug delivery, bio-sensing, magnetic fluid hyperthermia, and magnetic resonance imaging contrast enhancement [9]. Several studies have been carried out on the application of nanoparticles especially Fe_3O_4 nanoparticles in biomedicine. For instance, Kim et al. [10] reported

* Corresponding author.

E-mail addresses: ahrezayan@ut.ac.ir, ah_rezayan@yahoo.com (A.H. Rezayan).

that the monodisperse Fe_3O_4 nanoparticles could be conjugated to a breast cancer-targeting antibody, Herceptin, via 2,3-dimercapto-succinic acid and sulfosuccinimidyl-4-(*N*-maleimidomethyl) cyclohexane-1 carboxylate (sulfo-SMCC) and utilized as magnetic probes for breast cancer cell imaging applications [10–12].

The low solubility of iron oxide nanoparticle in aqueous solution and their destabilization due to the absorption of plasma proteins are perhaps the most significant constraints for their different applications. Magnetic nanoparticles agglomerates when exposed to physiology environment this could be attributed to increase in their surface area by severe interaction with plasma proteins. In these situations, the particles are removed from the blood circulation system and lose their function quickly. Moreover, nanoparticle based diagnostics and therapeutics have generally been tackled by the agglomeration of nanoparticles. One of the simplest and most effective remedies for this problem is the coating of nanoparticles with water solvable polymer such as PEG or Carboxylated polyethylenimine (PEI-COOH) [3,13,14].

Based on the aforementioned reasons and as a part of this study's ongoing research program, research design and synthesis of functionalized magnetic nanoparticles was conducted and their application in diagnosis and treatment were investigated [15–17]. In this study, the synthesis of monodisperse magnetite nanoparticles coated with water soluble polymers (Fe_3O_4 -DPA-PEG-COOH) for the diagnosis of breast cancer using MRI method (Fig. 1) was reported.

2. Experimental

2.1. Solvents and reagents

All reagents were used without further purification. However, all reagents and solvents were purchased from Merck (Germany) and Sigma-Aldrich Company.

2.2. Synthesis of magnetite nanoparticle (Fe_3O_4)

MNPs were prepared through co-precipitation process. First, an aqueous solution of $\text{Fe}^{3+}:\text{Fe}^{2+}$ with a molar ratio equal to 2:1 was

prepared by dissolving 2 mmol (0.54 g) $\text{FeCl}_3 \cdot 6\text{H}_2\text{O}$ and 1 mmol (0.19 gr) of $\text{FeCl}_2 \cdot 4\text{H}_2\text{O}$ in 100 ml deionized and deoxygenated water. Then this solution was ultrasonicated for about 30 mins under argon atmosphere. Thereafter, aqueous solution of NaOH (1.2 M) was added slowly to the solution and sonicated for extra 30 min. Finally, MNPs were magnetically separated and freeze dried to remove the solvent after 4 times washing with deionized water and ethanol (1:1).

2.3. Synthesis of PEG (2000) diacid (HOOC-PEG-COOH)

Briefly, 5 and 2.5 g PEG and succinic anhydride, respectively were dissolved in 25 ml dry toluene for up to one night at 70 °C. Then, the yielded PEG (2000) diacid was precipitated with hexane and dried using oven.

2.4. Coating Fe_3O_4 with HOOC-PEG-COOH via DPA linker (Fe_3O_4 -DPA-PEG-COOH)

PEG (2000) diacid (300 mg) was dissolved in a solution of CHCl_3 (15 mL), DMF (10 mL) containing NHS/DCC, dopamine hydrochloride (10.27 mg), and anhydrous Na_2CO_3 (100 mg). The solution was mechanically stirred at room temperature for 2 h. The solution of NPs was slowly added and followed by sonication for 15 mins under N_2 . After 24 h, the modified NPs were precipitated by adding hexane. The resulting NPs were separated by magnet and dried under N_2 . Finally, NPs were dissolved in deionized water and dialyzed using 12 kDa bag for 24 h in water.

3. Results and discussion

Fe_3O_4 -DPA-PEG-COOH nanoparticles were synthesized according to the synthetic route as shown in Fig. 1(a). In this study, PEG was used owing to its nontoxic nature and its ability to form a robust coating layer around nanoparticles, which provides a biocompatible and protective surface to keep nanoparticles from aggregating in physiologic environment and prohibition-specific uptake by reticular-endothelial system (RES) [9,18–22]. On the other hand, it has been proved that the DPA moiety has high

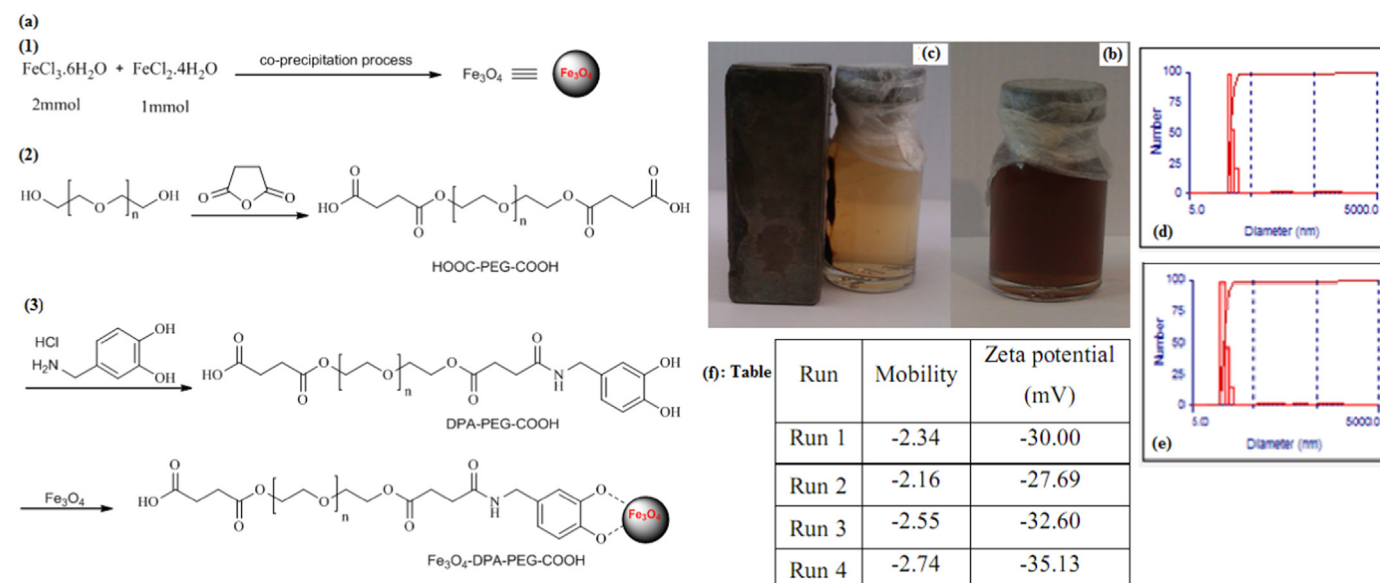


Fig. 1. Schematic synthesis of Fe_3O_4 -DPA-PEG-COOH nanoparticles, (a) Fe_3O_4 synthesis via co-precipitation method (1), Synthesis of PEG diacid (2), and immobilization of PEG diacid on Fe_3O_4 nanoparticles via DPA linker (3), (b) Visual image of nanoparticles in water, (c) Separation from solution using an external magnetic field, (d) Size distribution of nanoparticles in the absence of ultrasonic, (e) and also in the presence of ultrasonic and (f) Zeta potential value for the coated nanoparticles.

affinity for iron oxide shell of magnetic nanoparticles. A spectroscopic study by Rajh et al. [23] suggested that bidentate enediol ligands, such as DPA, convert the under-coordinated Fe surface sites back to a bulk-like lattice structure with an octahedral geometry for oxygen-coordinated iron, which may result in tight binding of DPA to iron oxide. The prepared Fe_3O_4 -DPA-PEG-COOH nanoparticles were fully characterized. Fig. 1(b) shows the visual image of nanoparticles in water and (c) its separation from solution using an external magnetic field.

3.1. Experimental X-ray diffraction analysis data

Determination of nanoparticles size was done by X-ray diffraction (XRD) which is presented in Fig. 2(a). XRD has a good potential for the analysis of nanostructures, because the diffraction patterns yield information about the building materials (sizes of crystallites, microstrain of a lattice, dis-location structures, etc.). There are numerous methods to analysis the X-ray diffraction line profiles. The most widely applied methods are the Scherrer, Williamson–Hall, and Warren–Aver–bach methods [24].

The diffraction patterns of the initial Fe nanopowder and reference are shown in Fig. 2(a). In comparison of the diffraction patterns of synthesized nanoparticles with diffraction patterns of the reference, the types of iron oxide sample could be recognized. Based on the analogy of the reference peaks, Fe_3O_4 and Fe_2O_3 could be found with maximum intensity values that are related to (311) planes. The second and third peaks (in view of intensity) in the diffraction pattern of materials have been located in different place. In the case of magnetite (Fe_3O_4), the second and third peaks were in (440) and (220) planes respectively, is contrary those of hematite (Fe_2O_3). In comparison of the diffraction pattern of the synthesized nanoparticles with reference patterns, the type of prepared iron oxide particles was found to be Fe_3O_4 .

The calculation of the size of synthesized nanoparticle was carried out using Scherrer method (Eq. (1)).

$$d = \frac{K\lambda}{B\cos\theta_0} \quad (1)$$

where λ is the radiation wavelength, B is the physical width of the reflection (in 2θ), θ_0 is the diffraction angle of the maximum line, and K is a constant close to unity ($K \approx 0.9$, if the half-width of a peak is taken, and $K \approx 1$ for the integral width) [24].

The calculations result using the Scherrer equation showed that the particle size was 10 nm.

3.2. Size distributions of nanoparticles

The size of the nanoparticles and their distribution is highly relevant to their method of synthesis. For instance, in the renowned co-precipitation method, the size distribution of nanoparticles is not homogeneous and as such, can affect the application of nanoparticles. However, co-precipitation method as the most used or popular method for the synthesis of nanoparticles is yet to be reported. One of the crucial parameters in co-precipitation method is the pH setting along particle formation, in which higher pH values leads to the formation of very small size of particle. In this study, pH=12.8 was used along with reaction during synthesis. The particle size distribution curve is shown in Fig. 1(d). According to particle size distribution curve, the average diameter of nanoparticles is 24 nm.

Ultrasonic was used to obtain the homogeneous particle. This technique will provide very uniform and narrow particle size distributions with good efficiency. The particle size distribution curve in the presence of ultrasonic waves is shown in Fig. 1(e). It can be concluded that the average particle size is 16 nm, which confirm the ultrasonic's clue effect.

3.3. Zeta potential analysis

For more consideration, zeta potential was measured. Zeta potential analysis is a technique that is used to obtain more

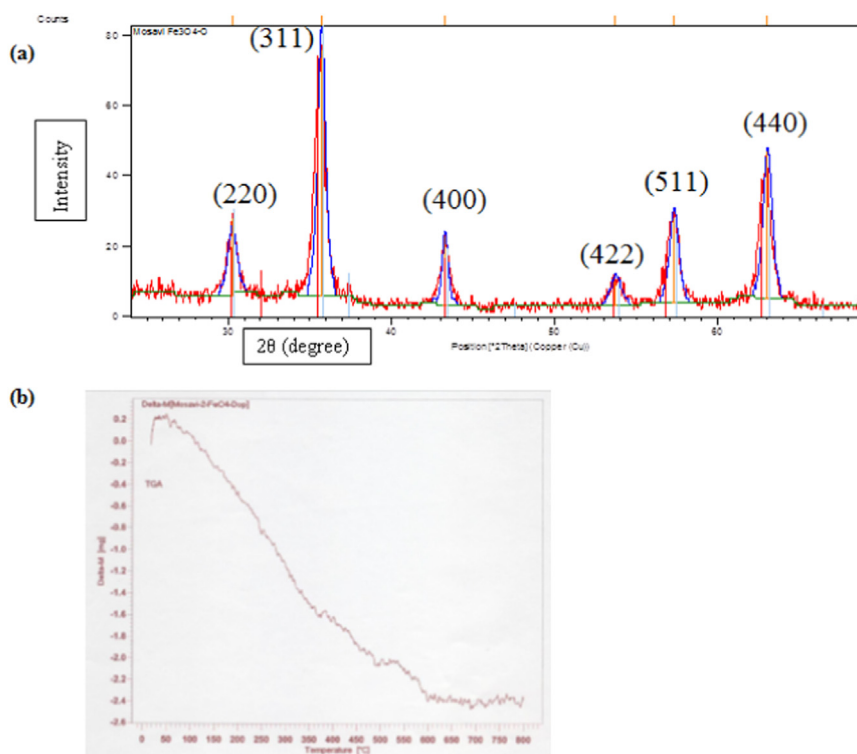


Fig. 2. (a) X-ray diffraction and (b) thermogravimetric analysis of Fe_3O_4 -DPA-PEG-COOH nanoparticle.

information about the colloidal stability through the determination of surface charge. Nanoparticles with zeta potential values greater than +25 mV or less than −25 mV typically have high rating of stability. In this study, in order to determine the surface charge of a coated nanoparticles, zeta potential was measured as shown in Fig. 1(f). As expected, nanoparticles had a negative surface charge (−27.69 mV to −35.13 mV), which could be attributed to the presence of end carboxyl groups of the polymer on the nanoparticle surface. There was a close agreement between the obtained results of this study and results previously reported by Wei et al. [25].

3.4. Thermogravimetric analysis (TGA)

For more characterization of the obtained nanoparticles, thermogravimetric analysis was performed on PEGdiacid-grafted

Fe_3O_4 nanoparticles. Fig. 2(b) shows that the weight loss in the timeframe of 100–200 °C was due to the desorption of water molecules from the surface, which was estimated to be about 5%. It can be concluded that the polymer inhibit water withdrawal. In the timeframe of 200–600 °C, weight loss was occurred different rates this could be attributed to the removal and desorption of immobilized polymeric matrix along with dopamine. About 22% was estimated as weight loss of PEGdiacid-grafted Fe_3O_4 nanoparticle [26].

3.5. FT-IR analysis

Fig. 3(a) shows the FT-IR spectra of pure Fe_3O_4 nanoparticle. As it is shown in Fig. 3(a), absorption peak at 567 cm^{-1} belongs to the stretching vibration mode of Fe–O bonds in Fe_3O_4 . The FT-IR spectrum of dopamine hydrochloride is shown in Fig. 3(b).

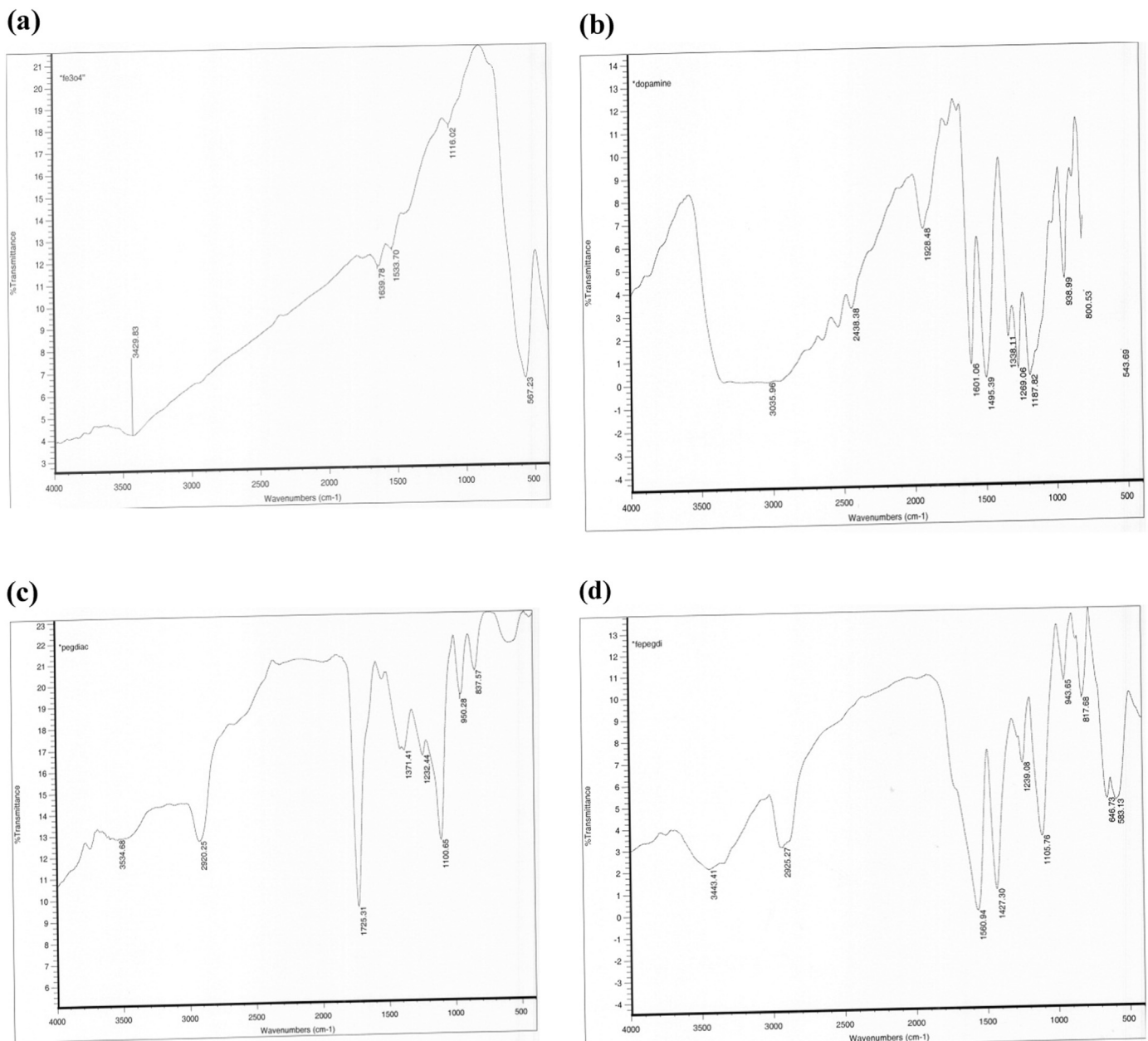


Fig. 3. FT-IR spectra of (a) pure Fe_3O_4 nanoparticles, (b) Dopamine hydrochloride, (c) PEGdiacid, (d) Fe_3O_4 -DPA-PEG-COOH nanoparticles.

After the carboxylation of PEG, in the polymer chain, all OH group were replaced by COOH. To assess the PEGdiacid, the polymer was participated using hexane and dried in an oven. The spectrum of PEGdiacid is shown in Fig. 3(c). The absorption peaks of 1725 cm^{-1} was associated with acidic C=O, indicating that the carboxylation of PEG had been done successfully.

The IR spectrum of the coated Fe_3O_4 nanoparticle (Fig. 3(d)) had absorption peaks of 1560 cm^{-1} being relevant to the stretching vibration of acidic C=O. These results confirmed the presence of acidic group on the coated nanoparticles. In comparison with the IR spectrum of PEGdiacid, in this wavelength, broadening could be observed, which may be due to the presence of dopamine aromatic ring. Moreover, the absorbent peak centered at 1105 and 2925 cm^{-1} can be attributed to the C–O–C bond and asymmetric stretching of CH bond, respectively. These results completely in line with the results obtained by Wei et al. [25]. Also, there was an adsorption band at 1427 cm^{-1} , which corresponds to the bending vibrations of CH_2 group. Therefore, these FT-IR spectra demonstrated that carboxylated polyethylene glycol (PEG-COOH) was successfully grafted onto the Fe_3O_4 nanoparticles surface.

3.6. Analysis of magnetic properties

Iron oxide nanoparticles have diversity of size and structure, leading to variation of magnetic properties. In this study, the coating process occurred in more than one step: first, the magnetic properties of the synthesized nanoparticle were measured in order to be sure of the super paramagnetic properties of the pure Fe_3O_4 nanoparticles. It was found that the saturation magnetizations (M_s) of the coated nanoparticles were more than the pure ones. Fig. 4 shows the magnetization curves of the pure Fe_3O_4 nanoparticles. As shown in Fig. 4, the pure Fe_3O_4 nanoparticles have super paramagnetic properties.

It is worthy of note that the use of a non-magnetic material for coating may cause mitigation in the magnetic properties of nanoparticles. The reduction of magnetic properties of nanoparticles in the presence of polyvinyl alcohol or starch as a coating agent has been reported previously by Voit et al. [26]. Sun et al. [27] also reported that the magnetic properties were mitigated at 90 to 15 emu/g when the coating material was amorphous silica. As shown in Fig. 4, the saturation magnetization (M_s) is 45 emu/g for PEGdiacid-modified Fe_3O_4 , which is less than the pure Fe_3O_4 nanoparticles (70 emu/g). This difference indicates that PEGdiacidpolymer was successfully immobilized on the surface of Fe_3O_4 nanoparticles.

3.7. Magnetic nanoparticles as contrast agents for MRI

Since the superparamagnetic Fe_3O_4 nanoparticles induce decrease in transverse relaxation time T_2 , leading to an increase in

contrast of the MRI images, the influence of PEG-grafted MNPs was investigated in terms of MR signal-enhancing property.

In order to evaluate the role of magnetic nanoparticles as a contrast agent, MRI imaging was carried out in defined protocol and in different concentration of nanoparticles. Fig. 3 show that the MR signal intensity is different for the different concentrations of MNPs. As shown in Fig. 5(a), it can be concluded that increase in the concentration of nanoparticles result in a decrease in transverse relaxation time T_2 , thus leading to MR signal enhancement.

For a systematic evaluation of the T_2 -weighted MRI images, the experiment was carried for different values of TE. Fig. 5(b) shows the T_2 -weighted MRI images for the different concentrations of MNPs in different values of echo time TE. This figure indicates that MR signal intensity increases with increase in TE value up to 66 and then remains constant.

As it is well known, the efficiency of the MRI contrast agent is measured via the frequency dependence of the transverse r_2 and longitudinal r_1 relaxivities defined by:

$$R_i = \left(-1/(T_i|_{\text{dia}}) + 1/(T_i|_{\text{meas}}) \right) / C_i = 1, 2$$

where C is the concentration of the magnetic center in mmol/L or mg/ml, $1/T_i|_{\text{dia}}$ is the relaxation rate of the nuclei in the diamagnetic host and $1/T_i|_{\text{meas}}$ is the relaxation rate measured in the presence of the CA [3,28]. The relaxation rates $1/T_2$ as a function of the iron molar concentration for the PEGdiacid-coated MNPs are shown in Fig. 6. As seen in the figure, the r_2 value of the PEGdiacid-grafted MNPs is $171.15\text{ mM}^{-1}\text{ s}^{-1}$, which is larger than that reported by Endorem [29]. In this study, the high value of r_2 is attributed to the high saturation magnetizations value. In considering the sufficient reduction in T_2 , it can be said that MNPs have significant potential to cause a negative contrast in MRI imaging.

3.8. Evaluation of cytotoxicity of PEGdiacid-grafted MNPs

The cytotoxicity of nanoparticles can be regarded as one of the important physicochemical properties [30]. Since the physicochemical properties of nanoparticle could be different depend on their different types, it is expected to have variable toxic effects on the cells. The toxic effect of nanoparticles can be reversible or permanent, which may lead to death of cell [30,31]. There are various tremendous tools for the measurement of cytotoxicity of nanoparticles. In this study, the MTT assay was carried out in order to evaluate the cytotoxic effect of the different concentrations of nanoparticles. This method is simple, repeatable, and it can be tailored for any assay without a radioisotopic requirement. The measurement was done for three different concentrations of nanoparticles (12 , 60 and 312 mg l^{-1}) at 24 and 48 h . Fig. 7 shows the cytotoxicity curve relative to different concentrations of Fe_3O_4 nanoparticles at various iron concentrations with and without

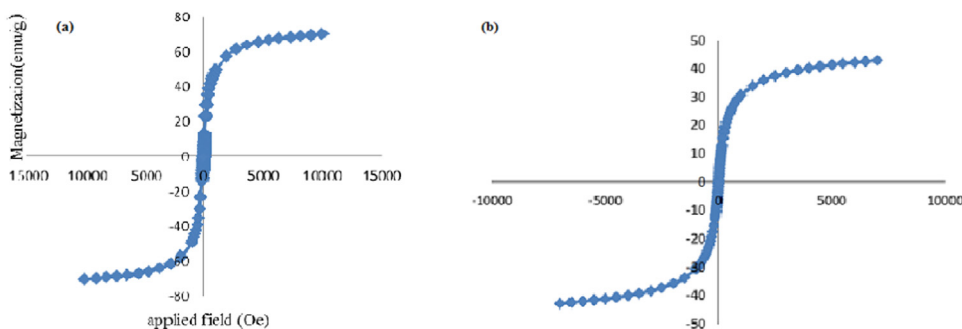


Fig. 4. Magnetization curves of (a) pure Fe_3O_4 nanoparticles and (b) PEGdiacid-modified Fe_3O_4 nanoparticles.

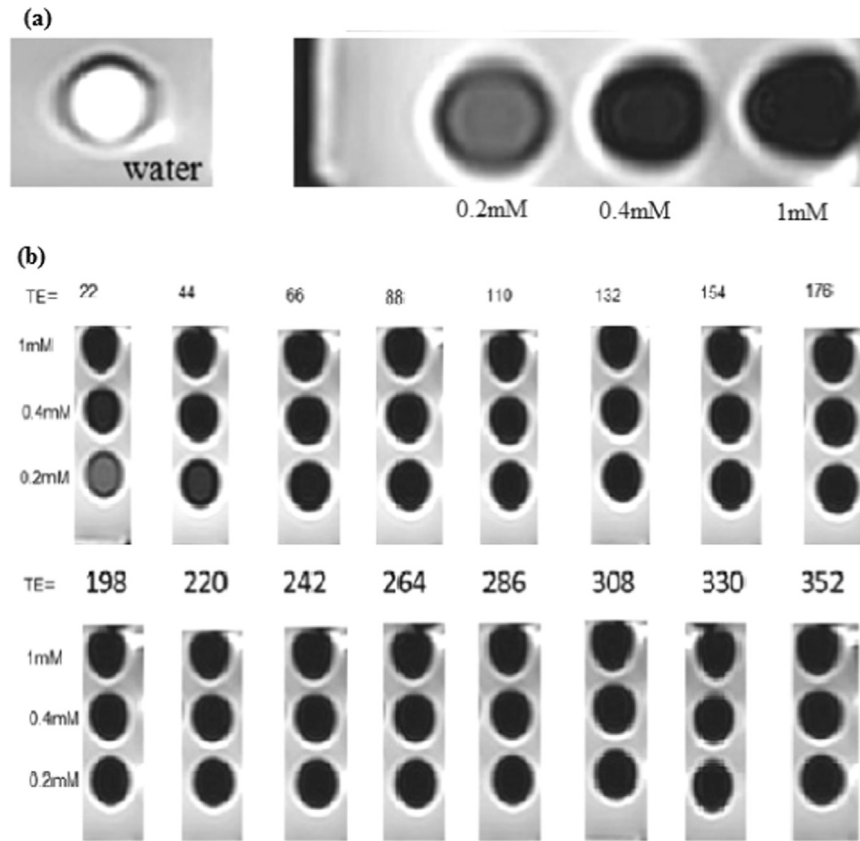


Fig. 5. (a) T_2 -weighted MRI images for three sample tubes with different concentrations of MNPs (echo time $TE=22$ ms) and (b) T_2 -weighted MRI images for the different concentrations of MNPs for the different values of echo time TE .

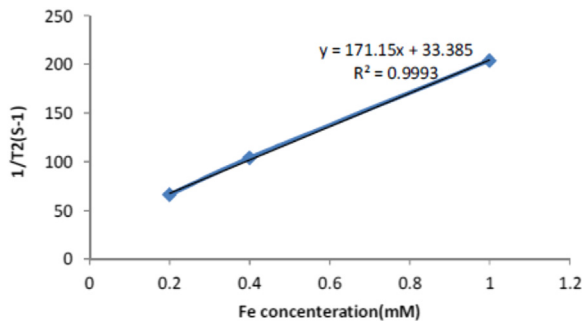


Fig. 6. The relaxation rates $1/T_2$ as a function of the iron molar concentration for the PEGdiacid-coated MNPs.

polymer grafting. As shown in Fig. 7, in both tested time (24 and 48 h) for all three samples, nanoparticle with PEGdiacid coating had a long life time than the pure Fe_3O_4 nanoparticles. For instance, this study obtained relatively 20 and 55 of the survival rate of cell after 24 h in 312 mg/L of the unmodified and polymer-grafted nanoparticles, respectively. In the other word, PEGdiacid-grafted Fe_3O_4 nanoparticles were less toxic and more biocompatible due to the increasing hydrodynamic size and decreasing chemical reactivity. Moreover, this polymer coating could be useful in the biocompatibility of nanoparticles by the prevention of additional oxidation of magnetite and Fe ions leakage.

As shown in Fig. 8(a), in the case of unmodified Fe_3O_4 nanoparticles after 24 h, at highest concentration of Fe_3O_4

nanoparticles, toxicity was observed, but in lower concentration of Fe, cell viability was up to 70%. However, in the interaction of cell with PEGdiacid-grafted Fe_3O_4 nanoparticles, toxicity dramatically dropped even in high concentration of Fe_3O_4 nanoparticles. The cytotoxicity effect of nanoparticles on high concentration of Fe_3O_4 nanoparticles could be due to DNA damage, which has been demonstrated by Karlsson et al. [32].

As shown in Fig. 8(b), after 48 h, cell viability was mitigated so that by exploiting the unmodified Fe_3O_4 nanoparticles, cytotoxicity effect would be intensive, resulting in death of cell except in very low concentration of Fe_3O_4 nanoparticles. But PEGdiacid-grafted Fe_3O_4 nanoparticles showed completely different effects of cytotoxicity behavior on the cell. The results were so promising, since toxicity was detectable only in the presence of the highest concentration of Fe_3O_4 nanoparticles.

3.9. Cell uptake

Breast cancer cells (MDA-MB-231) were obtained from the Pasteur Institute of Iran. 5×10^6 cells were cultured in DMEM with 10% FBS at 37 °C and 5% CO_2 atmosphere. The MDA-MB-231 cells were exposed to modified and unmodified MNPs. After 2 h, cells were separated via centrifuge and digested in HNO_3/HCl . The Fe_3O_4 nanoparticles concentrations within the cells were measured using the inductive coupled plasma – atomic emission spectrometry (ICP-AES) analysis. The particle surface charge and size showed significant impact on the uptake mechanisms. Cell uptake of PEGdiacid-grafted Fe_3O_4 NPs was 80–85% compared to unmodified NPs, which was 9–13%. Most unmodified NPs remained in solution and only 9% of them penetrated to the cells.

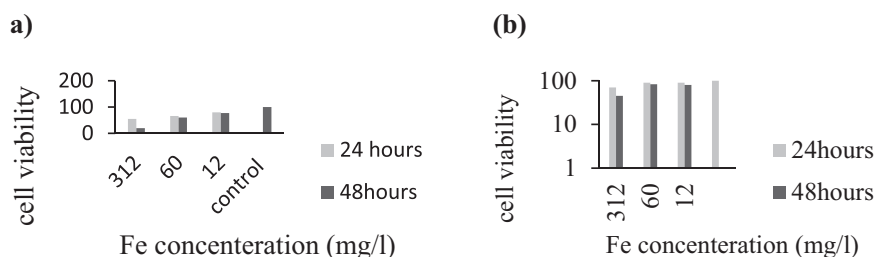


Fig. 7. Survival rate of cell for (a) pure Fe₃O₄ nanoparticles and (b) PEGdiacid-grafted Fe₃O₄ nanoparticles, in various concentrations of Fe after 24 and 48 h.

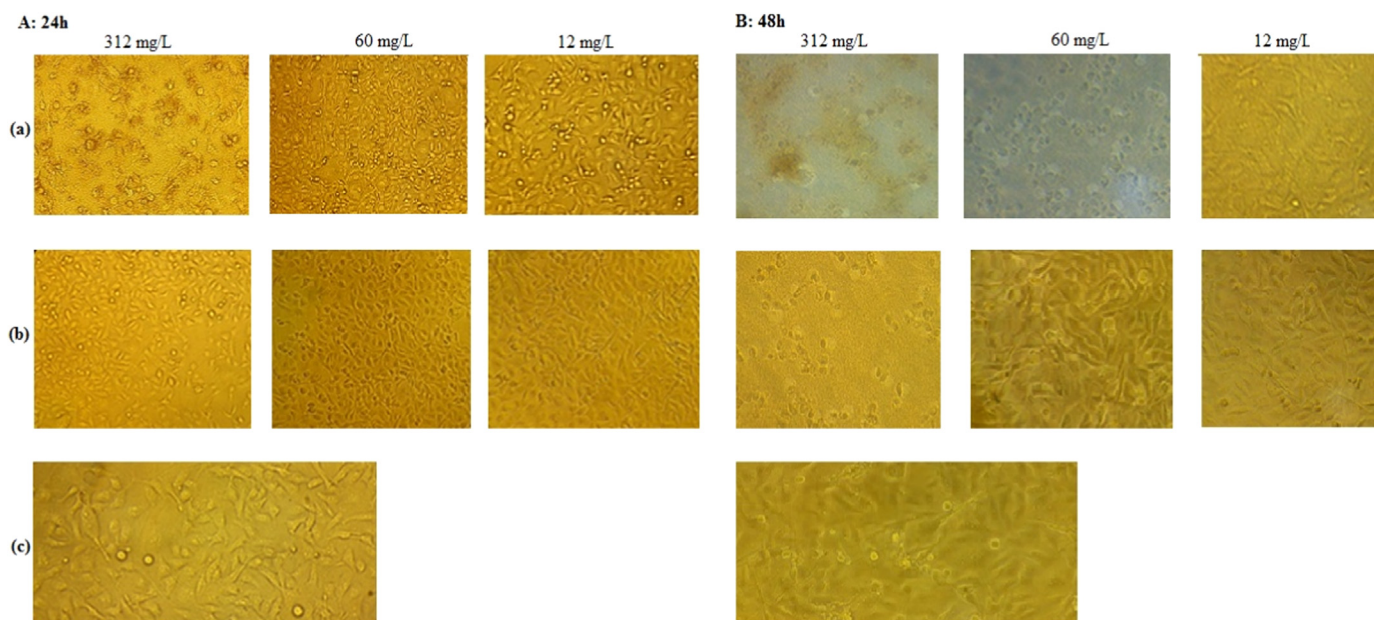


Fig. 8. Cell interaction with (a) pure Fe₃O₄ nanoparticles, (b) PEGdiacid-grafted Fe₃O₄ nanoparticles and (c) control sample after 24 h (A) and 48 h (B).

This may be attributed to serve agglomeration of the unmodified nanoparticles.

4. Conclusions

In the present study, a method for immobilizing of the macromolecule on the Fe₃O₄ nanoparticle surface was described. As mentioned in earlier, co-precipitation method was used for the synthesis of superparamagnetic Fe₃O₄ nanoparticles. However, before the grafting of the desired polymer on the surface, carboxylation of PEG was carried out using NHS/DCC and thereafter, the immobilization of PEGdiacid on the surface of MNPs was performed using DPA. The obtained results showed that the surface modification of Fe₃O₄ nanoparticles by polymer chain was more effective. The modified nanoparticles were superparamagnetic and completely stable and dispersible in water. The evaluation of the results of the different tests, such as concentration of MNPs on T2, value of echo time TE, cytotoxicity effect and cellular uptake on MDA-MB-231 breast cancer cells, showed that PEGdiacid-grafted Fe₃O₄ nanoparticles were the most effective contrast agent in MRI. On the other hand, it can be concluded from the calculated r_2 relaxivities that the PEGdiacid-grafted Fe₃O₄nanoparticles could be a tremendous entrant as T₂ contrast agent.

Acknowledgment

The authors would like to acknowledge the Iran National Science Foundation (INSF) for the financial support of this work (Project 90004726).

References

- [1] S. Mornet, S. Vasseur, F. Grasset, E. Duguet, Magnetic nanoparticle design for medical diagnosis and therapy, *J. Mater. Chem.* 14 (2004) 2161–2175.
- [2] Q.A. Pankhurst, J. Connolly, S.K. Jones, J. Dobson, Applications of magnetic nanoparticles in biomedicine, *J. Phys. D: Appl. Phys.* 36 (2003) R167–R181.
- [3] M. Corti, A. Lascialfari, M. Marinone, A. Masotti, E. Micotti, F. Orsini, G. Ortaggi, G. Poletti, C. Innocenti, C. Sangregorio, Magnetic and relaxometric properties of polyethylenimine-coated superparamagnetic MRI contrast agents, *J. Magn. Magn. Mater.* 320 (2008) e316–e319.
- [4] a) P.V. Prasad, N.J. Totowa, Magnetic resonance imaging: methods and biologic applications, in: *Methods in Molecular Medicine*, first ed., Springer, 2006.; b) M.G. Lansberg, M. Straka, MRI profile and response to endovascular reperfusion after stroke (DEFUSE 2): a prospective cohort study, *Lancet Neurol.* 11 (2012) 860–867.
- [5] S. Guo, D. Li, L. Zhang, J. Li, E. Wang, Monodisperse mesoporous superparamagnetic single-crystal magnetite nanoparticles for drug delivery, *Biomaterials* 30 (2009) 1881–1889.
- [6] Y. Zhang, N. Kohler, M. Zhang, Surface modification of superparamagnetic magnetite nanoparticles and their intracellular uptake, *Biomaterials* 23 (2002) 1553–1561.
- [7] M. Mahmoudi, S. Sant, B. Wang, S. Laurent, T. Sen, Superparamagnetic iron oxide nanoparticles (SPIONs): development, surface modification and applications in chemotherapy, *Adv. Drug. Deliv. Rev.* 63 (2011) 24–46.

- [8] H.M. Yang, C.W. Park, T. Ahn, B. Jung, B.K. Seo, J.H. Park, J.D. Kim, A direct surface modification of iron oxide nanoparticles with various poly(amino acid)s for use as magnetic resonance probes, *J. Colloid Interface Sci.* 391 (2013) 158–167.
- [9] a) X. Jin, X. Chenjie, X. Zhichuan, H. Yanglong, L. Kaylie, S.X. Young, N. Wang, Linking hydrophilic macromolecules to monodisperse magnetite (Fe_3O_4) nanoparticles via trichloro-s-triazine, *Chem. Mater.* 18 (2006) 5401–5403; b) V. Chandra, J. Park, Y. Chun, J. Woo Lee, In-Chul Hwang, Kwang S. Kim, Water-dispersible magnetite-reduced graphene oxide composites for arsenic removal, *ACS Nano* 4 (2010) 3979–3986; c) M. Faraji, Y. Yamini, M. Rezaee, Magnetic nanoparticles: synthesis, stabilization, functionalization, characterization, applications, *J. Iran. Chem. Soc.* 7 (2010) 1–37; d) A. Akbarzadeh, M. Samiei, S. Davaran, Magnetic nanoparticles: preparation, physical properties, and applications in biomedicine, *Nanoscale Res. Lett.* 7 (2010) 144–156; e) G. Mandarano, J. Lodhia, P. Eu, N.J. Ferris, R. Davidson, S.F. Cowell, Development and use of iron oxide nanoparticles (Part 2): the application of iron oxide contrast agents in MRI, *Biomed. Imaging Interv. J.* 6 (2010) e13–e27.
- [10] X. Jin, X. Chenjie, K. Nathan, H. Yanglong, S. Shouheng, Controlled PEGylation of monodisperse Fe_3O_4 nanoparticles for reduced non-specific uptake by macrophage cells, *Adv. Mater.* 19 (2007) 3163–3166.
- [11] Y.W. Jun, Y.M. Huh, J.S. Choi, J.H. Lee, H.T. Song, S. Kim, S. Yoon, K.S. Kim, J. S. Shin, J.S. Suh, J. Cheon, Nanoscale size effect of magnetic nanocrystals and their utilization for cancer diagnosis via magnetic resonance imaging, *J. Am. Chem. Soc.* 127 (2005) 5732–5733.
- [12] M.D. Butterworth, L. Illum, Preparation of ultrafine silica- and PEG-coated magnetite particles, *Colloids Surf. A* 179 (2001) 93–102.
- [13] A.F. Puentes, K.M. Krishnan, A.P. Alivisatos, Colloidal nanocrystal shape and size control: the case of cobalt, *Science* 291 (2001) 2115–2117.
- [14] Z. Yancong, Z. Lianying, S. Xinfeng, G. Xiangling, S. Hanwen, F. Chunhua, M. Fanzong, Synthesis of superparamagnetic iron oxide nanoparticles modified with MPEG-PEI via photochemistry as new MRI contrast agent, *J. Nanomater.* 2015 (2015) 1–6.
- [15] M. Shakourian-Fard, A.H. Rezayan, S. Kheirjou, A. Bayat, M.M. Hashemi, Synthesis of α -aminophosphonates in the presence of a magnetic recyclable $\text{Fe}_3\text{O}_4/\text{SiO}_2\text{-2mmsO}_3\text{H}$ nanocatalyst, *Bull. Chem. Soc. Jpn.* 87 (2014) 982–987.
- [16] X. Chenjie, X. Keming, G. Hongwei, Z. Rongkun, L. Hui, Z. Xixiang, G. Zhihong, X. Bing, Dopamine as a robust anchor to immobilize functional molecules on the iron oxide shell of magnetic nanoparticles, *J. Am. Chem. Soc.* 126 (2004) 9938–9939.
- [17] M. Amanlou, S.D. Siadat, S.E. Sadat Ebrahimi, A. Alavi, M.R. Aghasadeghi, M. Shafiee Ardestani, S. Shanehsaz, M. Ghorbani, B. Mehravi, M. Shafiee Alavideh, A. Jabbari-Arabzadeh, M. Abbasi, Gd^{3+} -DTPA-DG: novel nanosized dual anticancer and molecular imaging agent, *Int. J. Nanomed.* 6 (2011) 747–763.
- [18] K.S. Kim, S.H. Cho, J.S. Shin, Preparation and characterization of monodisperse polyacrylamide microgels, *Polym. J.* 27 (1995) 508–514.
- [19] R. Gref, M. Luck, P. Quellec, M. Marchand, S. DellacherieHarnisch, T. Blunk, R. H. Muller, 'Stealth' corona-core nanoparticles surface modified by polyethylene glycol (PEG): influences of the corona (PEG chain length and surface density) and of the core composition on phagocytic uptake and plasma protein adsorption, *Colloids Surf. B* 18 (2000) 301–313.
- [20] J.Milton Harris, Poly(ethylene glycol) Chemistry: Biotechnical and Biomedical Applications, Springer, New York, 1992.
- [21] M. Ogris, S. Brunner, S. Schuller, R. Kircheis, PEGylated DNA/transferrin-PEI complexes: reduced interaction with blood components, extended circulation in blood and potential for systemic gene delivery, *Gene Ther.* 6 (1999) 595–605.
- [22] P. Kingshott, H.J. Griessner, Surfaces that resist bioadhesion, *Curr. Opin. Solid State M4* (1999) 403–412.
- [23] a) T. Rajh, L.X. Chen, K. Lukas, T. Liu, M.C. Thurnauer, D.M. Tiede, Surface restructuring of nanoparticles: an efficient route for ligand–metal oxide crosstalk, *J. Phys. Chem. B* 106 (2002) 10543–10552; b) L.X. Chen, T. Liu, M.C. Thurnauer, R. Csencsits, T. Rajh, Fe_2O_3 nanoparticle structures investigated by X-ray absorption near edge structure, surface modifications, and model calculations, *J. Phys. Chem. B* 106 (2002) 8539–8546.
- [24] G.A. Dorofeev, A.N. Streletsii, I.V. Povstugar, A.V. Protasov, E.P. Elskov, Determination of nanoparticle sizes by X-ray diffraction, *Colloid J.* 74 (2012) 710–720.
- [25] B. Fenga, R.Y. Honga, L.S. Wang, L. Guoc, H.Z. Li, J. Dingd, Y. Zhenge, D.J. Wei, Synthesis of Fe_3O_4 /APTES/PEG diacid functionalized magnetic nanoparticles for MR imaging, *Colloids Surf. A* 328 (2008) 52–59.
- [26] W. Voit, D.K. Kim, W. Zapka, M. Muhammed, K.V. Rao, Magnetic behavior of coated superparamagnetic iron oxide nanoparticles in ferrofluids, *Mater. Res. Soc. Symp. Proc.* 676 (2001), Y7.8.1–Y7.8.6.
- [27] S.A. Gomez-Lopera, R.C. Plaza, A.V. Delgado, Synthesis and characterization of spherical magnetite/biodegradable polymer composite particles, *J. Colloid Interface Sci.* 240 (2001) 40–47.
- [28] P. Carretta, A. Lascialfari, NMR-MRI, μSR and Mossbauer Spectroscopies in Molecular Magnets, Springer, New York, 2007.
- [29] C.W. Jung, P. Jacobs, Physical and chemical properties of superparamagnetic iron oxide MR contrast agents: ferumoxides, ferumoxtran, ferumoxsil, *Magn. Reson. Imaging* 13 (1996) 661–674.
- [30] B. Venugopal, A.A. Hajarul, S. Shaharum, In vitro evaluation of cytotoxicity of colloidal amorphous silica nanoparticles designed for drug delivery on human cell lines, *J. Nanomater.* 2013 (2013) 1–8.
- [31] J.M. Hillegass, A. Shukla, S.A. Lathrop, M.B. Mac Pherson, N.K. Fukagawa, B. T. Mossman, Assessing nanotoxicity in cells in vitro, *WIREs, Nanomed. Nanobiol.* 2 (2010) 219–231.
- [32] H.L. Karlsson, P. Cronholm, J. Gustafsson, L. Moller, Copper oxide nanoparticles are highly toxic: a comparison between metal oxide nanoparticles and carbon nanotubes, *Chem. Res. Toxicol.* 21 (2008) 1726–1732.